miR-155 induces endothelial cell apoptosis and inflammatory response in atherosclerosis by regulating Bmal1

SHUANGCHAO LIANG[1,2], JIQIONG HU[2], ANDONG ZHANG[2], FANGKUAN LI[2] and XIAOQIANG LI[1]

[1]Department of Vascular Surgery, The Second Affiliated Hospital of Soochow University, Suzhou, Jiangsu 215000; [2]Department of Vascular Surgery, Yijishan Hospital of Wannan Medical College, Wuhu, Anhui 241000, P.R. China

Received December 19, 2019; Accepted June 18, 2020

DOI: 10.3892/etm.2020.9259

Abstract. Atherosclerosis is the leading cause of death from vascular diseases worldwide, and endothelial cell (EC) dysfunction is the key cause of atherosclerosis. *miR-155* was found to induce endothelial injury and to trigger atherosclerosis. In addition, brain and muscle ARNT-like protein-1 (Bmal1) has been found to be closely related to EC function. Therefore, the present study aimed to explore the mechanism underlying the regulation of Bmal1 by *miR-155* in the induction of EC apoptosis and inflammatory response in atherosclerosis. The atherosclerosis model in apolipoprotein E (ApoE)$^{-/-}$ mice was established. *miR-155* and Bmal1 expression was quantified by RT-qPCR and western blot analysis, respectively. The role of *miR-155* and Bmal1 in atherosclerosis was evaluated through changes in cardiac function, plaque area, cardiomyocyte apoptosis, and inflammatory factor levels in mice. Moreover, the regulatory relationship between them was identified by dual-luciferase reporter gene assay to explore the mechanism of action of *miR-155*. After the modeling, the expression of *miR-155* was upregulated and Bmal1 was downregulated in aorta, and there was a significant linear correlation between them. Upregulation of *miR-155* increased the atherosclerotic plaque area, cell apoptosis, total cholesterol (TC) and triglyceride (TG), as well as weakened aortic diastolic function. However, opposite changes occurred after downregulation of *miR-155* or an increase in Bmal1. In addition, the microRNA.org website predicted that there were targeted binding sites between *miR-155* and Bmal1, which was verified with a dual-luciferase reporter gene assay. *miR-155* was able to inhibit the expression by targeting Bmal1. Moreover, a rescue experiment showed that Bmal1 hindered the promotion of *miR-155* in regards to atherosclerosis. In conclusion, *miR-155* induces EC apoptosis and inflammatory response, weakens aortic diastolic function, and promotes the progression of atherosclerosis through targeted inhibition of Bmal1.

Correspondence to: Dr Xiaoqiang Li, Department of Vascular Surgery, The Second Affiliated Hospital of Soochow University, 1055 Sanxiang Road, Suzhou, Jiangsu 215000, P.R. China
E-mail: liangchao.0000@163.com

Key words: miR-155, Bmal1, atherosclerosis, endothelial cells, inflammatory response

Introduction

Atherosclerosis, a chronic arterial disease characterized by ischemic heart disease (IHD), ischemic stroke and peripheral arterial disease, is the leading cause of death from vascular diseases worldwide (1,2). The number of individuals who died of IHD accounts for about 30% of the global death toll per year (3). In 2016, there were 11 million individuals suffering from IHD in China; IHD will become the leading cause of disability and death by 2020 (4).

Endothelial cell (EC) dysfunction is the key cause of atherosclerosis, mainly manifested in complete exfoliation and dysfunction of the endothelial monolayer caused by EC apoptosis, leading to lipid accumulation and inflammation and atherosclerotic lesions (5,6). MicroRNAs (miRNAs/miRs), a class of single-stranded short non-coding RNAs (approximately 17-22 bp) are involved in almost all biological processes, and regulate the translation and degradation of targeted mRNAs by binding to their 3'-untranslated region (UTR). It has been suggested that targeting miRNAs is a promising therapeutic method for cancer (7,8). Studies also suggest the role of *miR-155* in regulating EC function. Zheng *et al* (9) reported that *miR-155* induces endothelial injury and triggers atherosclerosis. Yang *et al* (10) demonstrated that *miR-155* plays a role in controlling hypoxia inducible factor 1α (HIF-1α) expression under hypoxia and promotes angiogenesis, which is also a key feature of mature ECs. However, the role of *miR-155* in ECs needs further investigation. Brain and Muscle ARNT-like protein-1 (Bmal1), also called aryl hydrocarbon receptor nuclear translocator like (ARNTL), with the coding gene is located on human chromosome 11p15.3. It is closely related to EC function regulation and promotes angiogenesis by regulating vascular endothelial growth factor A (VEGF-A) (11). In addition, Zhu *et al* found that Bmal1 inhibited endothelial-mesenchymal transformation, and its deletion accelerated atherosclerosis progression and enhanced plaque stability (12). Whether *miR-155* and Bmal1 are valuable in atherosclerosis is not fully understood. It was previously reported that *miR-155* could target Bmal1 to regulate the circadian rhythm of macrophages, reducing the plasma cholesterol level of patients with early atherosclerosis, but inducing inflammatory response at the same time (13,14).

The present study analyzed the effects of *miR-155* and Bmal1 on ECs of atherosclerotic mice to elaborate the mechanism underlying *miR-155* and Bmal1 in atherosclerosis and provides further experimental basis for potential target searching.

Materials and methods

Mice. Eighty C57BL/6 apolipoprotein E-deficient ($ApoE^{-/-}$) mice [SCXK (Guizhou) 2018-0001] were purchased from the Experimental Animal Center of Guizhou Medical University. The mice (6 weeks old, weighing 18-22 g) were maintained at room temperature of 20-25˚C, relative humidity of 40-70%, light/dark cycle of 12 h, and had free access to food and water. All animal experiments were approved by the Animal Ethics Committee of The Second Affiliated Hospital of Soochow University and followed the guidelines of the Council for International Organizations of Medical Sciences (CIOMS) (15).

Modeling and grouping. Ten C57BL/6 $ApoE^{-/-}$ mice served as the blank group, and 70 $ApoE^{-/-}$ mice were randomly allocated into an inhibitor group, inhibitor-NC group, mimic group, mimic-NC group, Bmal1 group, Bmal1-NC group, and combination group (10 mice in each group). The blank group received no treatment, and the inhibitor group, mimic group, Bmal1 group and combination group were treated with *miR-155* inhibitor, *miR-155* mimic, recombinant Bmal1 plasmid and *miR-155* mimic+recombinant Bmal1 plasmid, respectively, while the inhibitor-NC group, mimic-NC group and Bmal1-NC group were given their own vector controls. *miR-155* inhibitor, *miR-155* mimic, recombinant Bmal1 plasmid and vector controls were all designed and synthesized by Thermo Fisher Scientific, Inc., and the plasmid applied was PGL3-promoter. The following are the sequences: *miR-155* mimics sequence, 5'-UUAAUGCUAAUUGUGAUAGGG GU-3' and mimic-NC sequence, 5'-UUCUCCGAACGUGUC ACGUTT-3'; *miR-155* inhibitor sequence, 5'-ACCCCUAUC ACGAUUAGCAUUAA-3' and inhibitor-NC sequence, 5'-CAG UACUUUUGUGUAGUACAA-3'. After pre-treatment with Liposome 2000 (Invitrogen; Thermo Fisher Scientific, Inc.), the concentration of mimic and inhibitor used was adjusted to 50 mg/kg, and tail vein injection (100 μl) was performed once every 4 weeks. All mice were fed with a high-fat diet containing 0.15% cholesterol and 21% fat. After 16 weeks, intervention effect was observed. The mice were anesthetized with pentobarbital (60 mg/kg), and were sacrificed by cervical dislocation to collect corresponding specimens.

Blood lipid test. Heart blood samples (2 ml) from the mice were centrifuged at 1,000 x g at 4˚C for 15 min, and the total cholesterol (TC) and triglyceride (TG) levels in serum were detected using a Roche MODULAR P800 automatic biochemical analyzer (Roche Diagnostics).

Diastolic function test. After the mice were sacrificed, the tissues around the aorta were removed. A 4-mm long vascular ring was connected to a JH-2 force transducer. A arterial ring was placed in a constant temperature isolated tissue and organ perfusion system (HV-4, Techman, Chengdu, China) containing Krebs-Hensleit's solution, with a tension load of 2 x g. After 1 h, the arterial ring was pre-stimulated with norepinephrine ($1x10^{-6}$ mol/l). After the tension was balanced, acetylcholine at different concentrations (10^{-9}, 10^{-8}, 10^{-7}, 10^{-6}, 10^{-5}, 10^{-4} mol/l) was used to stimulate the arterial ring again. BL-420S biological signal recording system was employed to record the tension of the arterial ring in each group. Equipment and related reagents were provided by Chengdu TECHMAN Technology Co., Ltd.

Plaque area detection. A 2-mm aorta was excised from the aortic arch to the bifurcation of the common iliac artery, fixed on a glass slide using 4% paraformaldehyde with the endothelium upward, and then stained for 4 h with Oil Red O. Controlnetics (Silver Spring, MD, USA) was used to calculate the positive staining rate (plaque area/total aortic area). The relevant reagents were all purchased from Thermo Fisher Scientific, Inc.

Apoptosis detection. The apoptotic rate was detected by TdT-mediated dUTP nick end labeling (TUNEL) staining. After the aorta sample was frozen and sectioned, TUNEL reagent was applied for staining at 37˚C for 1 h. For specific steps, please refer to the instruction manual of the TUNEL kit (Thermo Fisher Scientific, Inc.; KHO1001).

Inflammatory factor detection. Levels of serum tumor necrosis factor (TNF)-α and interleukin-6 (IL-6) were measured by enzyme-linked immunosorbent assay (ELISA). Biotinylated anti-mouse TNF-α or IL-6 was added to antibody-coated microwells, followed by incubation at room temperature for 2 h. After washing, HRP conjugated streptavidin was added and incubated at room temperature for 1 h. After another washing, tetramethyl benzidine (TMB) solution was added, and incubated at room temperature for 10 min. Following addition of stop solution, color development was carried out at 620 nm. Relevant kits were all purchased from Thermo Fisher Scientific, Inc. (cat. nos. BMS622 and CRC0063).

Reverse transcription-quantitative polymerase chain reaction (RT-qPCR). Total RNA of the aortic arch was extracted using a TRIzol kit. The MiRNeasy Micro kit was used to extract total RNA from exosomes. The purity, concentration, as well as integrity of the extracted total RNA were determined using an ultraviolet spectrophotometer and agarose gel electrophoresis (28s/18s ≥2 and 1.8< A260/A280 value <2.1. One-step RNA amplification was adopted with a reaction system containing 1 μg of RNA Template, 0.4 μl of Forward GSP (10 μM), 0.4 μl of Reverse GSP (10 μM), 10 μl of 2X One-Step Reaction Mix, 0.4 μl of Easy Script One-Step Enzymmix, and RNase-Free water supplemented to 20 μl. The reaction conditions were: 40˚C for 30 min, 94˚C for 5 min, 94˚C for 30 sec, 60˚C for 30 sec, 72˚C for 2 kb/min, 72˚C for 10 min, a total of 42 cycles. Glyceraldehyde-3-phosphate-dehydrogenase (GAPDH) and U6 served as the internal reference for long non-coding RNA (lncRNA) and miRNA, respectively. The TRIzol kit was purchased from Invitrogen; Thermo Fisher Scientific, Inc. (cat. no. 15596018), EasyScript One-Step RT-PCR SuperMix kit was purchased from Beijing TransGen (cat. no. AE411-02), and the microplate reader was purchased from Shanghai Flash Spectrum. Primer sequences were

Table I. Primer sequences.

	Forward primer	Reverse primer
miR-155	5'-CGTTAATGCTAATCGTGATAG-3'	5'-GCAGGGTCCGAGGT-3'
U6	5'-GCGCGTCGTGAAGCGTTC-3'	5'-GTGCAGGGTCCGAGGT-3'

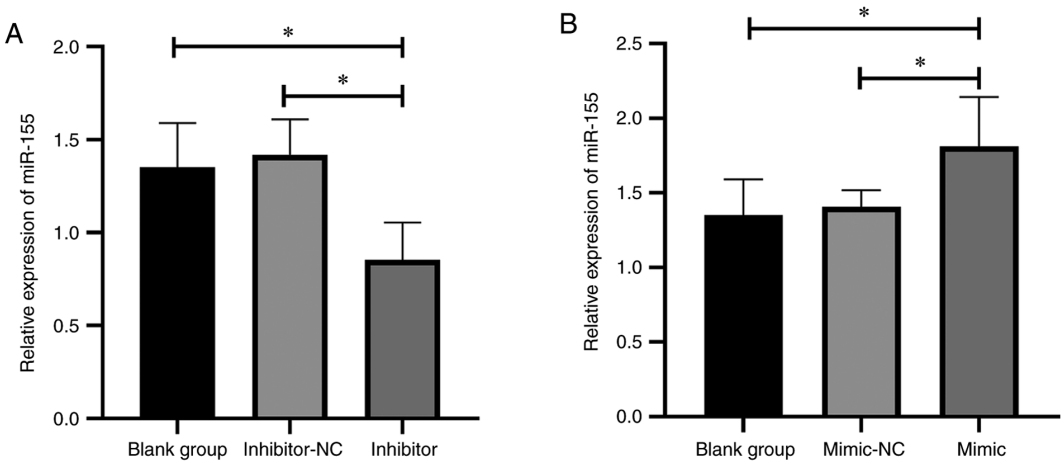

Figure 1. Outcomes of the miR-155 intervention. (A) Effect of miR-155 inhibitor on miR-155 expression. (B) Effect of miR-155 mimic on miR-155 expression. *P<0.05. miR, microRNA; NC, negative control.

designed and synthesized by Thermo Fisher Scientific, Inc. (China) (Table I).

Western blot analysis. Proteins were extracted from aortic arch by repeated freezing and thawing, and the concentration was detected with bicinchoninic acid (BCA) method and adjusted to 4 μg/μl. The proteins were separated by 12% polyacrylamide gel electrophoresis. The initial voltage was 90 V, which was then increased to 120 V to move the sample to the appropriate position on separating gel. Afterwards, proteins were transferred to a polyvinylidene fluoride membrane (Amersham Pharmacia Biotech) at a constant voltage of 100 V for 100 min, then blocked for 60 min. Afterwards, the membrane was blocked in 5% skimmed milk powder, and then immune reaction was carried out. The membrane was incubated overnight with primary antibody (dilution 1:1,000) at 4˚C and washed three times with phosphate-buffered saline (PBS) on the next day, 5 min each time, and then incubated with secondary antibody (dilution 1:1,000) for 1 h at room temperature. Subsequently, enhanced chemiluminescence (ECL) reagent was used for developing and fixing. The protein bands scanned were statistically analyzed by Quantity One Software 1-D (Bio-Rad Laboratories, Inc.), and the relative expression of protein=gray value of target band/gray value of internal reference. BCA protein kit (cat. no. 23250), ECL kit (cat. no. 35055) and trypsin (cat. no. 90058) were all purchased from Thermo Fisher Scientific, Inc. Rabbit anti-Bmal1 polyclonal antibody (cat. no. ab3350) and goat anti-rabbit IgG secondary antibody (cat. no. ab6721) were purchased from Abcam.

Dual-luciferase reporter gene assay. Primer sequences were all designed and synthesized by Thermo Fisher Scientific, Inc. (China). 293T cells in logarithmic growth phase were transfected with pmirGLO-Bmal1-3'UTR wild-type (Wt), pmirGLO-Bmal1-3'UTR mutant (Mut), *miR-155* mimics, *miR-155* inhibitor, and miR-NC, respectively. The fluorescence intensity was measured 48 h after transfection with dual-luciferase reporter gene assay (Promega Corporation). Data were normalized by β-galactosidase.

Statistical analysis. Graphpad Prism 8 (GraphPad Software, Inc.) was employed to statistically analyze and visualize the data. All trials were repeated three times. Measurement data are expressed as mean ± standard deviation (SD). One-way analysis of variance (ANOVA) was used for multi-group comparison, Fisher's least significant difference (LSD) test for post-hoc test, independent samples t-test for between-group comparison, and Pearson test for correlation analysis. P<0.05 was considered to indicate a statistically significant difference.

Results

Outcomes of the miR-155 intervention. The mice receiving *miR-155* inhibitor intervention showed significantly decreased *miR-155* compared with those in the blank group (P<0.05; Fig. 1A). The mice receiving *miR-155* mimic intervention showed significantly increased *miR-155* (P<0.05; Fig. 1B). There was no significant difference in *miR-155* expression between the inhibitor-NC and mimic-NC groups.

Outcomes of Bmal1 intervention. The mice receiving recombinant Bmal1 plasmid presented significantly increased Bmal1 compared with those in the blank group (P<0.05), and there was no significant difference in Bmal1 expression between the Bmal1

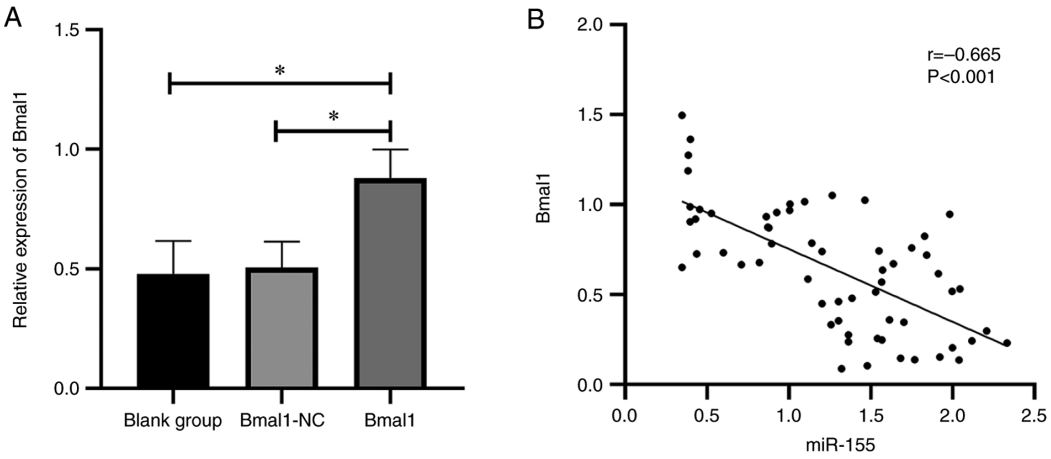

Figure 2. Outcomes of Bmal1 intervention. (A) Effect of recombinant Bmal1 plasmid on Bmal1 expression. (B) Correlation analysis between miR-155 and Bmal1 expression. *P<0.05. miR, microRNA; Bmal1, brain and muscle ARNT-like protein-1.

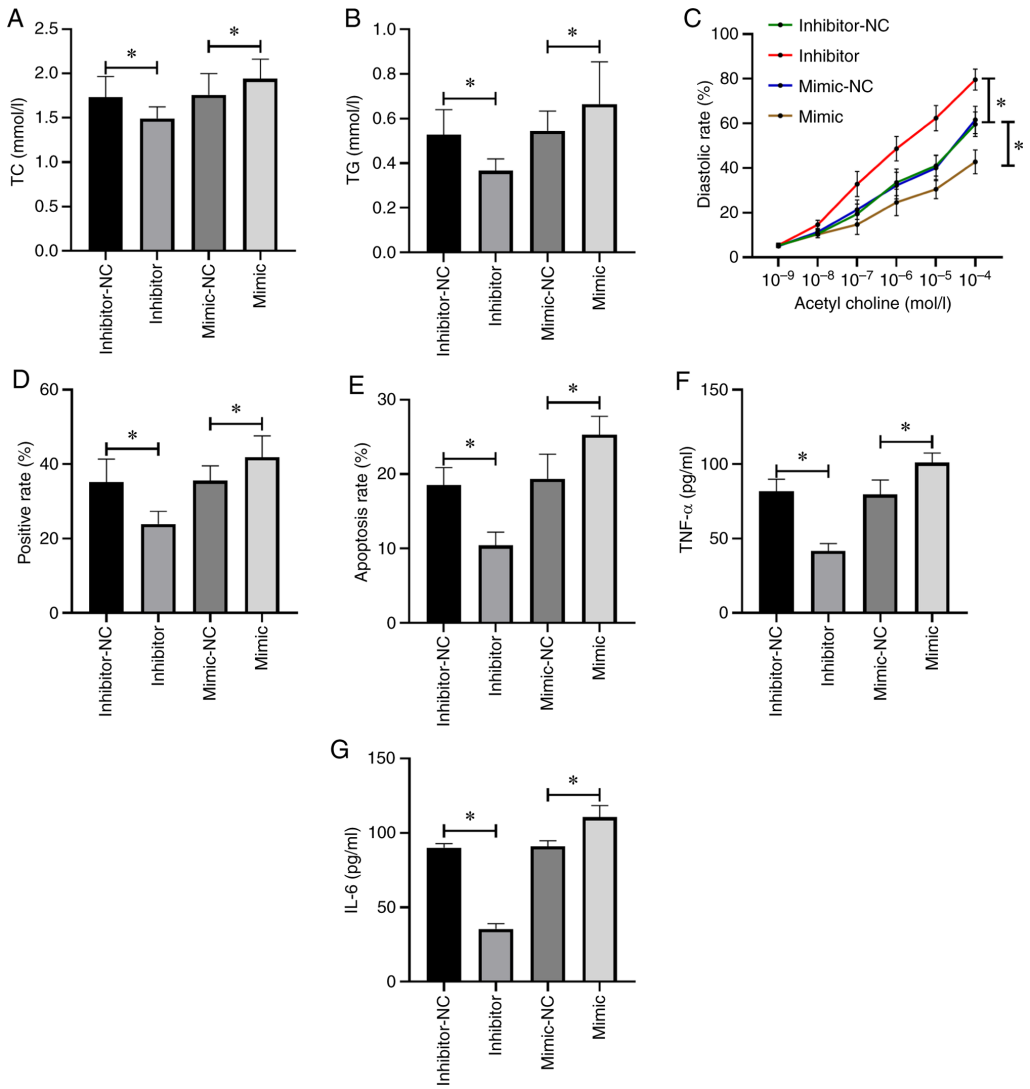

Figure 3. Effects of miR-155 on atherosclerosis. (A) Changes in TC level in mice. (B) Changes in TG level in mice. (C) Changes in aortic diastolic function in mice. (D) Changes in aortic plaque area in mice. (E) Changes in the apoptotic rate in mice. (F) Changes in TNF-α in mice. (G) Changes in IL-6 in mice. *P<0.05. TC, total cholesterol; TG, total triglyerides; IL-6, interleukin-6; TNF, tumor necrosis factor; miR, microRNA; NC, negative control.

group and blank group (P>0.05; Fig. 2A). Moreover, *miR-155* was found to be negatively correlated with Bmal1 (Fig. 2B).

Effects of miR-155 on atherosclerosis. The mice receiving *miR-155* inhibitor intervention had decreased TC (Fig. 3A),

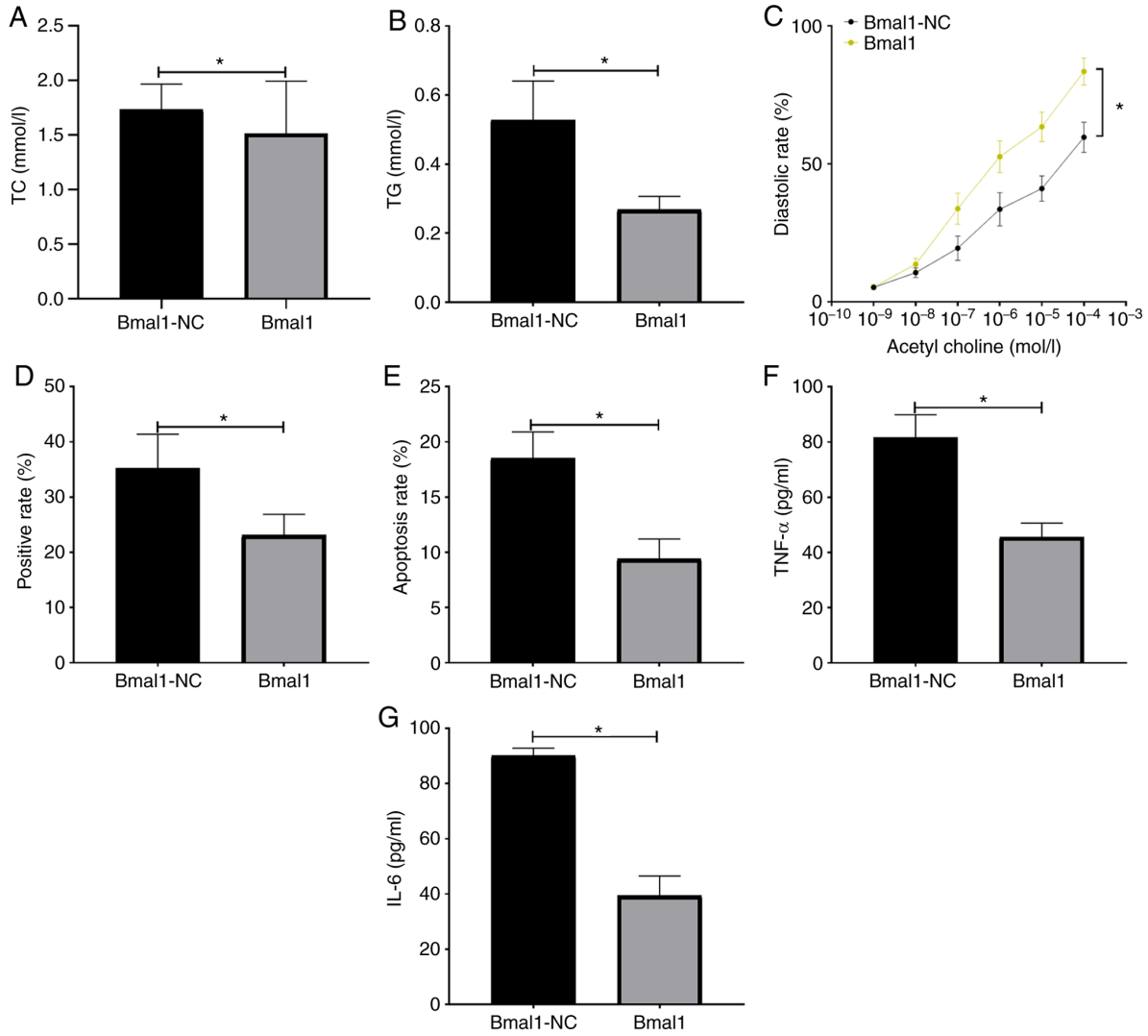

Figure 4. Effects of Bmal1 on atherosclerosis. (A) Changes in TC level in mice. (B) Changes in TG level in mice. (C) Changes in aortic diastolic function in mice. (D) Changes in aortic plaque area in mice. (E) Changes in the apoptotic rate in mice. (F) Changes in TNF-α in mice. (G) Changes in IL-6 in mice. *P<0.05. Bmal1, brain and muscle ARNT-like protein-1; TC, total cholesterol; TG, total triglyerides; IL-6, interleukin-6; TNF, tumor necrosis factor; miR, microRNA; NC, negative control.

TG (Fig. 3B), TNF-α (Fig. 3F) and IL-6 levels (Fig. 3G), as well as aortic plaque area (Fig. 3D) and apoptotic rate (Fig. 3E) than those in the control group (P<0.05), and aortic diastolic function was enhanced (P<0.05; Fig. 3C). However, the mice receiving *miR-155* mimic intervention demonstrated completely opposite results (P<0.05; Fig. 3).

Effects of Bmal1 on atherosclerosis. The mice receiving recombinant Bmal1 plasmid had decreased TC (Fig. 4A), TG (Fig. 4B), TNF-α (Fig. 4F), IL-6 levels (Fig. 4G), as well as aortic plaque area (Fig. 4D) and apoptotic rate (Fig. 4E) than those in the Bmal1-NC group (P<0.05), and aortic diastolic function was enhanced (P<0.05; Fig. 4C).

Effects of Bmal1 on the role of miR-155. The expression of *miR-155* in the combination group was not different from that in the mimic group (P>0.05), but higher than that in the Bmal1 group (P<0.05; Fig. 5A). The expression of Bmal1 in the combination group was higher than that in the mimic group (P>0.05), but lower than that in the Bmal1 group (Fig. 5B) (P<0.05). Compared with mimic group, the TC (Fig. 5C), TG (Fig. 5D), TNF-α (Fig. 5H), IL-6 (Fig. 5I), aortic plaque area (Fig. 5F) and apoptotic rate (Fig. 5G) were lower and aortic diastolic function (Fig. 5E) was enhanced in the combination group (P<0.05). When compared with the Bmal1 group, the results were reversed (P<0.05; Fig. 5).

Dual-luciferase reporter gene assay. Targeted binding sites between *miR-155* and Bmal1 were predicted by TargetScan (16). The results of cell transfection in each group are shown in Fig. 6A. The fluorescence intensity of 293T cells transfected with *miR-155* mimic was significantly decreased (P<0.05), while the intensity of those transfected with *miR-155* inhibitor was significantly increased (P<0.05; Fig. 6).

Discussion

Vascular response in atherosclerosis is a process involving ECs, macrophages, and smooth muscle cells. ECs trigger vascular endothelial injury under various stimuli, causing failure of the

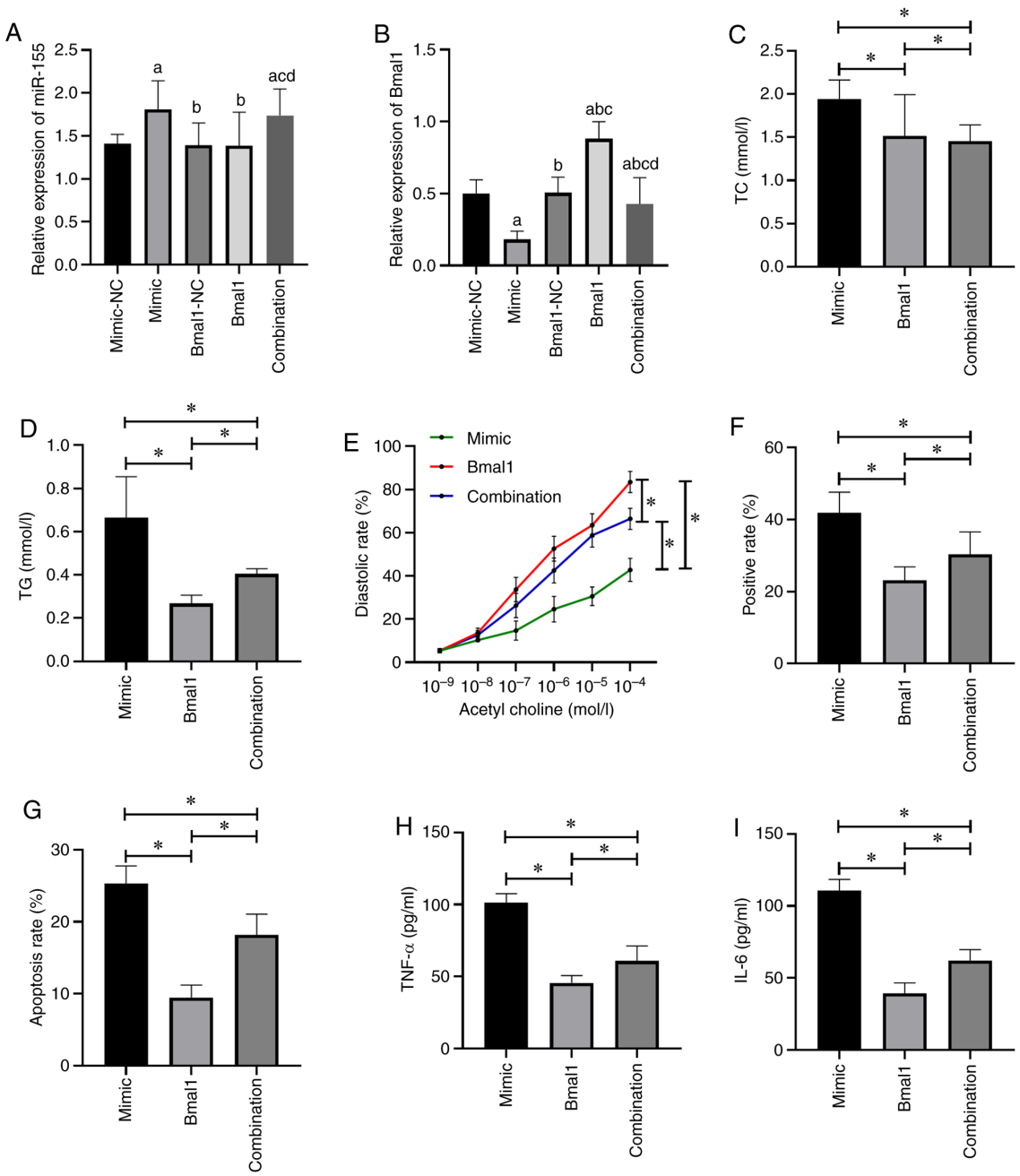

Figure 5. Effects of Bmal1 on the role of miR-155. (A) Expression level of miR-155. (B) Expression level of Bmal1. [a]P<0.05 vs. mimic-NC group, [b]P<0.05 vs. mimic group, [c]P<0.05 vs. Bmal1-NC group, [d]P<0.05 vs. Bmal1 group. (C) Changes in TC level in mice. (D) Changes in TG level in mice. (E) Changes in aortic diastolic function in mice. (F) Changes in the aortic plaque area in mice. (G) Changes in the apoptotic rate in mice. (H) Changes in TNF-α in mice. (I) Changes in IL-6 in mice. *P<0.05. Bmal1, brain and muscle ARNT-like protein-1; TC, total cholesterol; TG, total triglyerides; IL-6, interleukin-6; TNF, tumor necrosis factor.

endothelium to regulate lipid homeostasis, immune function, and inflammation, hence causing vascular smooth muscle cell activation and macrophage infiltration as well as accelerating the formation of atherosclerotic plaques (17-19). Therefore, strategies with which to reduce EC injury are the focus of research on the treatment of atherosclerosis. It has been emphasized that miRNAs are dysregulated in atherosclerosis, and they are also key factors in regulating EC function (20,21). Therefore, miRNA investigation is an important direction to identify targets for atherosclerosis.

We established atherosclerosis models with ApoE$^{-/-}$ mice and found abnormal expression of *miR-155* and Bmal1, which is similar to previous research findings (22,23). We artificially interfered with the expression of *miR-155* and Bmal1 in mice during modeling. As expected, *miR-155* and Bmal1 in the aorta of mice exhibited corresponding changes. Moreover, we found that there was a significant linear correlation between them. Elevated *miR-155* increased atherosclerotic plaque area, cell apoptosis, TC and total TG levels in mice, as well as weakened aortic diastolic function, while decreased *miR-155* or increased Bmal1 showed opposite results. This indicated that *miR-155* promoted and Bmal1 hindered the progression of atherosclerosis. According to Gomez *et al*, exosomes carrying *miR-155* released from neutrophils during vascular infiltration were fused with ECs, leading to vascular inflammation and atherosclerosis (24). Faccini *et al* also indicated the high

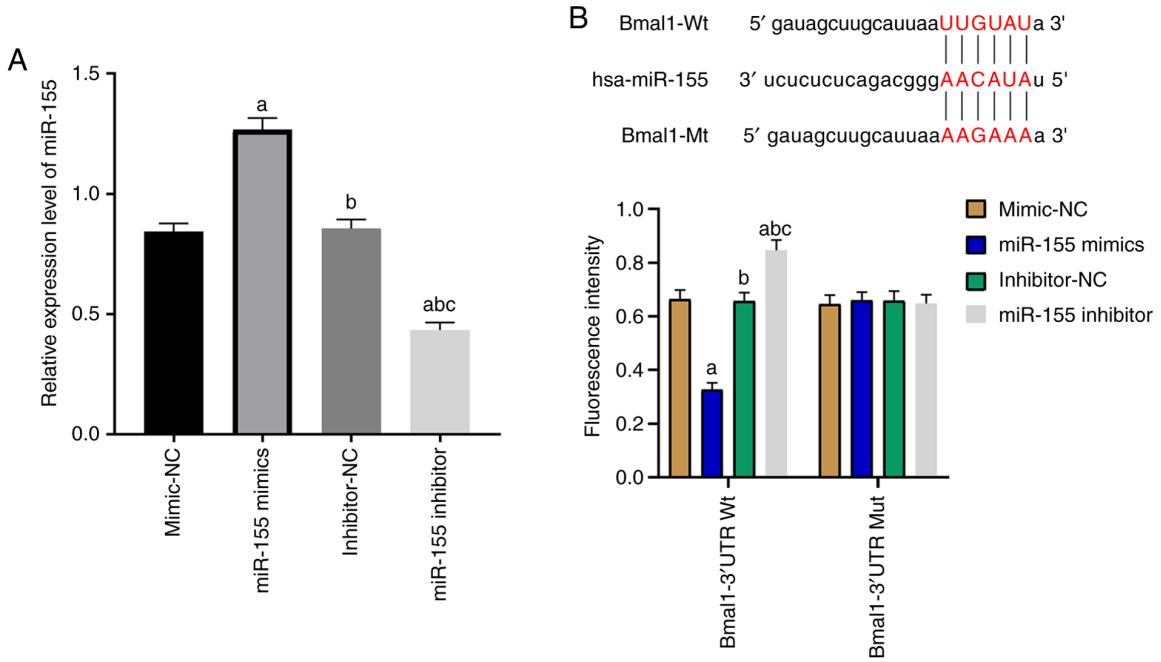

Figure 6. Dual-luciferase reporter gene assay. (A) Analyses of miR-155 mimic and miR-155inhibitor transfection. (B) Prediction of targeted binding sites between miR-155 and Bmal1 and evaluation of fluorescence intensity. [a]P<0.05 vs. mimic-NC group, [b]P<0.05 vs. miR-155 mimic group, [c]P<0.05 vs. inhibitor-NC group. miR, microRNA; NC, negative control.

diagnostic value of *miR-155* in coronary atherosclerosis (25). There were also studies that proposed that *miR-155* is a protective factor for atherosclerosis. Huang *et al* reported that overexpression of *miR-155* in peripheral blood mononuclear cells inhibited the inflammatory response (26). Moreover, Li *et al* found that *miR-155* relieved chronic inflammation in atherosclerosis through negative feedback regulation of nuclear factor (NF)-κB, and inhibited foam cell formation via calcium-regulated heat stable protein 1 signaling pathway, thus alleviating atherosclerosis (27). The above studies analyzed the role of *miR-155* in atherosclerosis from different aspects, indicating the diverse mechanisms of *miR-155*, which need to be explored by more scholars.

Concerning Bmal1, the currently accepted view is that it maintains vascular function and slows down the formation of atherosclerosis by regulating the circadian rhythm of intestinal flora and vascular cells (28). Moreover, it has been reported to play a role in regulating inflammation, for example, by modulating the macrophage inflammatory response (29), inhibiting local inflammation in arthritis (30), as well as suppressing cardiomyocyte inflammation and reducing cardiomyocyte apoptosis (31).

In the present study, the effects of *miR-155* and Bmal1 on the inflammatory response were investigated. Inflammation is an important manifestation of atherosclerosis characterized by macrophage infiltration. On the good side, macrophage infiltration is conducive to the restoration of damaged vessels (22), but the promotion of macrophages in regards to inflammatory factors, nitric oxide synthase, cyclooxygenase-2, and reactive oxygen species may lead to EC injury (32). In the present study, *miR-155* was found to alleviate the inflammatory response in atherosclerosis mice, while Bmal1 played an inhibitory role, which meant that *miR-155* and Bmal1 affect the development of atherosclerosis in many ways. We mentioned earlier that *miR-155* and Bmal1 expression were found to be negatively correlated, thus there may be a regulatory relationship between *miR-155* and Bmal1. Prediction results from the microRNA.org website demonstrated that *miR-155* and Bmal1 share targeted binding sites, which was verified by dual-luciferase reporter gene assay. *miR-155* was able to inhibit the expression of Bmal1 in a targeted manner. Moreover, a rescue experiment showed that Bmal1 hindered the *miR-155*-mediated promotion of atherosclerosis.

Atherosclerosis, an inflammatory disease of the arterial wall characterized by the formation of white blood cell-rich plaques in the intimal layer of large and medium-sized arteries, is induced and maintained by the inflow, proliferation and activation of immune cells (33,34). *miR-155* is reported to play a role in activating immune response and promoting T cell activation (35,36), indicating that *miR-155* may be involved in the enhancement of the immune response during atherosclerosis. Therefore, we preliminarily confirmed that *miR-155* promoted the development of atherosclerosis through targeted inhibition of Bmal1. However, the limitations of this study lie in the fact that ECs were not isolated, and only the apoptosis of ECs from stained frozen sections of aorta was investigated. Moreover, the regulatory relationship between *miR-155* and Bmal1 needs to be further verified by RNA immunoprecipitation, and the role of *miR-155* and Bmal1 in normal wild-type mice should also be explored. Many indicators, nitric oxide synthase, especially, have not been analyzed. Moreover, the relationship between *miR-155* and Bmal1 in atherosclerosis-related cells such as macrophages, smooth muscle cells, and dendritic cells needs to be further explored.

In conclusion, *miR-155* induces EC apoptosis and inflammatory response, weakens arterial diastolic function, and promotes the progression of atherosclerosis through the targeted inhibition of Bmal1.

Acknowledgements

Not applicable.

Funding

This work was supported by Open Subject Key Laboratory of Anhui University (RNA201905) and Natural Science Major Program of Anhui University (KJ2018ZD026).

Availability of data and materials

The datasets used and/or analyzed during the current study are available from the corresponding author on reasonable request.

Authors' contributions

SL conceived the study and drafted the manuscript. JH and AZ acquired the data. FL and XL analyzed the data and revised the manuscript. All authors read and approved the final manuscript.

Ethics approval and consent to participate

The study was approved by the Ethics Committee of The Second Affiliated Hospital of Soochow University, Suzhou, Jiangsu, China.

Patient consent for publication

Not applicable.

Competing interests

The authors declare that they have no competing interests.

References

1. Mujaj B, Bos D, Muka T, Lugt AV, Ikram MA, Vernooij MW, Stricker BH and Franco OH: Antithrombotic treatment is associated with intraplaque haemorrhage in the atherosclerotic carotid artery: A cross-sectional analysis of The Rotterdam Study. Eur Heart J 39: 3369-3376, 2018.
2. Linton MF, Yancey PG, Davies SS, Jerome WG, Linton EF, Song WL, Doran AC and Vickers KC: The role of lipids and lipoproteins in atherosclerosis. In: Endotext [Internet]. Feingold KR, Anawalt B, Boyce A, *et al* (eds). MDText.com, Inc., South Dartmouth, MA, 2019.
3. Du H, Li L, Bennett D, Guo Y, Key TJ, Bian Z, Sherliker P, Gao H, Chen Y, Yang L, *et al*: Fresh fruit consumption and major cardiovascular disease in China. N Engl J Med 374: 1332-1343, 2016.
4. Writing Group Members, Mozaffarian D, Benjamin EJ, Go AS, Arnett DK, Blaha MJ, Cushman M, Das SR, de Ferranti S, Després JP, *et al*: Executive summary: Heart disease and stroke statistics-2016 update: A report from the American Heart Association. Circulation 133: 447-454, 2016.
5. Menghini R, Casagrande V, Marino A, Marchetti V, Cardellini M, Stoehr R, Rizza S, Martelli E, Greco S, Mauriello A, *et al*: MiR-216a: A link between endothelial dysfunction and autophagy. Cell Death Dis 5: e1029, 2014.
6. Chen C, Cheng G, Yang X, Li C, Shi R and Zhao N: Tanshinol suppresses endothelial cells apoptosis in mice with atherosclerosis via lncRNA TUG1 up-regulating the expression of miR-26a. Am J Transl Res 8: 2981-2991, 2016.
7. Tutar L, Özgür A and Tutar Y: Involvement of miRNAs and pseudogenes in cancer. Methods Mol Biol 1699: 45-66, 2018.
8. Salehi M and Sharifi M: Exosomal miRNAs as novel cancer biomarkers: Challenges and opportunities. J Cell Physiol 233: 6370-6380, 2018.
9. Zheng B, Yin WN, Suzuki T, Zhang XH, Zhang Y, Song LL, Jin LS, Zhan H, Zhang H, Li JS and Wen JK: Exosome-mediated miR-155 transfer from smooth muscle cells to endothelial cells induces endothelial injury and promotes atherosclerosis. Mol Ther 25: 1279-1294, 2017.
10. Yang D, Wang J, Xiao M, Zhou T and Shi X: Role of Mir-155 in controlling HIF-1α level and promoting endothelial cell maturation. Sci Rep 6: 35316, 2016.
11. Burgermeister E, Battaglin F, Eladly F, Wu W, Herweck F, Schulte N, Betge J, Härtel N, Kather JN, Weis CA, *et al*: Aryl hydrocarbon receptor nuclear translocator-like (ARNTL/Bmal1) is associated with bevacizumab resistance in colorectal cancer via regulation of vascular endothelial growth factor A. EBioMedicine 45: 139-154, 2019.
12. Zhu M, Tang H, Tang X, Ma X, Guo D and Chen F: 1 suppresses ROS-induced endothelial-to-mesenchymal transition and atherosclerosis plaque progression via BMP signaling. Am J Transl Res 10: 3150-3161, 2018.
13. Curtis AM, Fagundes CT, Yang G, Palsson-McDermott EM, Wochal P, McGettrick AF, Foley NH, Early JO, Chen L, Zhang H, *et al*: Circadian control of innate immunity in macrophages by miR-155 targeting Bmal1. Proc Natl Acad Sci USA 112: 7231-7236, 2015.
14. Tabas I and Bornfeldt KE: Macrophage phenotype and function in different stages of atherosclerosis. Circ Res 118: 653-667, 2016.
15. Vallotton MB: Council for international organizations of medical sciences perspectives: Protecting persons through international ethics guidelines. Int J Integr Care 10 (Suppl): e008, 2010.
16. Agarwal V, Bell GW, Nam JW and Bartel DP: Predicting effective microRNA target sites in mammalian mRNAs. Elife 4: e05005, 2015.
17. Paone S, Baxter AA, Hulett MD and Poon IKH: Endothelial cell apoptosis and the role of endothelial cell-derived extracellular vesicles in the progression of atherosclerosis. Cell Mol Life Sci 76: 1093-1106, 2019.
18. Libby P, Bornfeldt KE and Tall AR: Atherosclerosis: Successes, surprises, and future challenges. Circ Res 118: 531-534, 2016.
19. Goetzl EJ, Schwartz JB, Mustapic M, Lobach IV, Daneman R, Abner EL and Jicha GA: Altered cargo proteins of human plasma endothelial cell-derived exosomes in atherosclerotic cerebrovascular disease. FASEB J 31: 3689-3694, 2017.
20. Brennan E, Wang B, McClelland A, Mohan M, Marai M, Beuscart O, Derouiche S, Gray S, Pickering R, Tikellis C, *et al*: Protective effect of let-7 miRNA family in regulating inflammation in diabetes-associated atherosclerosis. Diabetes 66: 2266-2277, 2017.
21. Gong M, Yu B, Wang J, Wang Y, Liu M, Paul C, Millard RW, Xiao DS, Ashraf M and Xu M: Mesenchymal stem cells release exosomes that transfer miRNAs to endothelial cells and promote angiogenesis. Oncotarget 8: 45200-45212, 2017.
22. Bruen R, Fitzsimons S and Belton O: miR-155 in the resolution of atherosclerosis. Front Pharmacol 10: 463, 2019.
23. Lindskog Jonsson A, Caesar R, Akrami R, Reinhardt C, Fåk Hållenius F, Borén J and Bäckhed F: Impact of gut microbiota and diet on the development of atherosclerosis in Apoe$^{-/-}$ mice. Arterioscler Thromb Vasc Biol 38: 2318-2326, 2018.
24. Gomez I, Ward B, Souilhol C, Recarti C, Ariaans M, Johnston J, Burnett A, Mahmoud M, Luong LA, West L, *et al*: Neutrophil microvesicles drive atherosclerosis by delivering miR-155 to atheroprone endothelium. Nat Commun 11: 214, 2020.
25. Faccini J, Ruidavets JB, Cordelier P, Martins F, Maoret JJ, Bongard V, Ferrières J, Roncalli J, Elbaz M and Vindis C: Circulating miR-155, miR-145 and let-7c as diagnostic biomarkers of the coronary artery disease. Sci Rep 7: 42916, 2017.
26. Huang J, Yang Q, He L and Huang J: Role of TLR4 and miR-155 in peripheral blood mononuclear cell-mediated inflammatory reaction in coronary slow flow and coronary arteriosclerosis patients. J Clin Lab Anal 32: e22232, 2018.
27. Li X, Kong D, Chen H, Liu S, Hu H, Wu T, Wang J, Chen W, Ning Y, Li Y and Lu Z: miR-155 acts as an anti-inflammatory factor in atherosclerosis-associated foam cell formation by repressing calcium-regulated heat stable protein 1. Sci Rep 6: 21789, 2016.
28. Wu X, Chen L, Zeb F, Li C, Jiang P, Chen A, Xu C, Haq IU and Feng Q: Clock-Bmal1 mediates MMP9 induction in acrolein-promoted atherosclerosis associated with gut microbiota regulation. Environ Pollut 252: 1455-1463, 2019.

29. Oishi Y, Hayashi S, Isagawa T, Oshima M, Iwama A, Shimba S, Okamura H and Manabe I: Bmal1 regulates inflammatory responses in macrophages by modulating enhancer RNA transcription. Sci Rep 7: 7086, 2017.
30. Hand LE, Dickson SH, Freemont AJ, Ray DW and Gibbs JE: The circadian regulator Bmal1 in joint mesenchymal cells regulates both joint development and inflammatory arthritis. Arthritis Res Ther 21: 5, 2019.
31. Ingle KA, Kain V, Goel M, Prabhu SD, Young ME and Halade GV: Cardiomyocyte-specific Bmal1 deletion in mice triggers diastolic dysfunction, extracellular matrix response, and impaired resolution of inflammation. Am J Physiol Heart Circ Physiol 309: H1827-H1836, 2015.
32. Butcher M and Galkina E: Current views on the functions of interleukin-17A-producing cells in atherosclerosis. Thromb Haemost 106: 787-795, 2011.
33. Winkels H, Ehinger E, Vassallo M, Buscher K, Dinh HQ, Kobiyama K, Hamers AAJ, Cochain C, Vafadarnejad E, Saliba AE, *et al*: Atlas of the immune cell repertoire in mouse atherosclerosis defined by single-cell RNA-sequencing and mass cytometry. Circ Res 122: 1675-1688, 2018.
34. Kusters PJH, Lutgens E and Seijkens TTP: Exploring immune checkpoints as potential therapeutic targets in atherosclerosis. Cardiovasc Res 114: 368-377, 2018.
35. Jin C, Cheng L, Lu X, Xie T, Wu H and Wu N: Elevated expression of miR-155 is associated with the differentiation of $CD8^+$ T cells in patients with HIV-1. Mol Med Rep 16: 1584-1589, 2017.
36. Jin C, Cheng L, Höxtermann S, Xie T, Lu X, Wu H, Skaletz-Rorowski A, Brockmeyer NH and Wu N: MicroRNA-155 is a biomarker of T-cell activation and immune dysfunction in HIV-1-infected patients. HIV Med 18: 354-362, 2017.